Case Studies in Thermal Engineering 8 (2016) 370–377

Contents lists available at ScienceDirect

Case Studies in Thermal Engineering

journal homepage: www.elsevier.com/locate/csite

Heat transfer behavior of flat plate having spherical dimpled surfaces

Nat Vorayos [a], Nopparat Katkhaw [a,*], Tanongkiat Kiatsiriroat [a], Atipoang Nuntaphan [b]

[a] Department of Mechanical Engineering, Chiang Mai University, Chiang Mai 50202, Thailand
[b] Thermal Technology Research Laboratory, Mae Moh Training Center, Electricity Generating Authority of Thailand, Mae Moh, Lampang 52220, Thailand

ARTICLE INFO

Article history:
Received 15 March 2016
Received in revised form
16 August 2016
Accepted 15 September 2016
Available online 20 September 2016

Keywords:
Vortex
Dimple
Enhanced heat transfer

ABSTRACT

In the present study, heat transfer analysis of dimpled surfaces of external flow was investigated. A total of 14 types of dimpled surfaces are studied. The effect of dimple pitch was examined. The experiments were carried out with air stream flows over the heated surface with dimples. The temperature and velocity of air stream and temperature of dimpled surfaces were measured. The heat transfer of dimpled surfaces was investigated and compared with the result of smooth surface. For the staggered arrangement, the computed results show that the maximum Nusselt number for dimpled surfaces are about 26% better than smooth surface. And for the inline arrangement, the results show that the maximum Nusselt number for dimples surfaces are about 25% better than smooth surface.

1. Introduction

The conventional heat transfer enhancement approaches to increase either the heat transfer rate or the turbulence of fluid stream, in general, it involves the incorporation of fins, baffles, turbulizers and etc. Although, these approaches are the effective method to improve the heat transfer performance; however, the increasing of fluid stream pressure drop should be concerned. The dimpled surface is one of the effective methods to improve the heat transfer rates without the significant pressure drop. Normally, the dimpled surface generates the vortex flow within its hole [1] and the augmentation of heat transfer is obtained.

In the early investigations, Afanasyev et al. [2], investigated the overall heat transfer rate and the pressure drop for a flat plate having shallow dimples under the turbulent flow of air stream. They found 30–40% increase of heat transfer performance with negligible pressure drop. Chyu et al. [3] presented the influences of the concavities imprinted on the surface in the staggered arrays. They found the augmentation of heat transfer rate around 2.5 times compared to the smooth surface.

Mahmood et al. [4] studied the flow structure above the dimpled surface by using flow visualization technique and numerical analysis. Their results showed the periodic and the continuous shedding of primary vortex pair from the central portion of the dimple and the secondary vortex pair shed from the span-wise edges of the dimple. Moreover, they found the heat transfer distribution and local Nusselt number variation on the dimpled surface. Their results showed the lower heat transfer region on the upstream half of the dimple cavity followed by the higher heat transfer region on the downstream

* Correspondence to: Department of Mechanical Engineering, School of Engineering, University of Phayao, Phayao 56000, Thailand.
E-mail address: nopparat_ka@hotmail.com (N. Katkhaw).

http://dx.doi.org/10.1016/j.csite.2016.09.004
2214-157X/

Nomenclature

A_s	Surface area (m^2)
D	Dimple diameter (mm)
h	Average heat transfer coefficient (W/m^2K)
h_x	Local heat transfer coefficient (W/m^2K)
h_0	Average heat transfer coefficient of flat plate without dimple (W/m^2K)
k_f	Thermal conductivity of air stream (W/mK)
L	Maxima stream-wise surface length (m)
Nu_L	Average Nusselt number base on a maxima stream-wise surface length
Nu_0	Baseline average Nusselt number of flat plate without dimple
Pr	Prandtl number
q''	Surface heat flux (W/m^2)
Re_L	Reynolds number base surface length (include dimples surface)
S_L	Streamwise pitch (mm)
S_T	Spanwise pitch (mm)
T_s	Surface temperature (°C)
T_∞	Temperature of inlet air (°C)
V_f	Velocity of air (m/s)
x	Spanwise coordinate
y	Streamwise coordinate

Greek symbols

ρ_f	Density of air (kg/m^3)
μ_f	Dynamic viscosity of air (Ns/m^2)

half. The additional regions of high heat transfer were identified at the downstream rim of the dimple.

Ligrani et al. [5] studied the flow structure of the dimpled channel and the effect of channel height on the vortex form. They found out that a primary vortex pair is periodically shed from the central portion of each dimple, including a large upwash region. This shedding occurs periodically and continuously, and is followed by inflow advection into the dimple cavity. As the ratio of channel height to dimple print diameter decreases, the strength of the primary vortex pair increases, and two additional secondary vortex pairs which form near the span-wise edges of each dimple become significantly stronger and larger in cross section.

Ligrani et al. [6] investigated the Nusselt numbers and flow structure on and above a shallow dimpled surface within a channel including the effects of inlet turbulence intensity level. They discover that the highest local Nusselt number ratios are presented within the downstream portions of dimples, as well as near dimple span-wise and downstream edges. Local and spatially averaged Nusselt number ratios sometimes change by small amounts as the channel inlet turbulence intensity level is altered, whereas friction factor ratios increase somewhat at the channel inlet turbulence intensity level increases. These changes to local Nusselt number data (with changing turbulence intensity level) are present at the same locations where the vortex pairs appear to originate, where they have the greatest influences on local flow and heat transfer behavior.

Burgess et al. [7] studied the effect of dimple depth on the Nusselt number and they reported that both the Nusselt number and the friction augmentation increased with the raising of dimple depth. These are attributed to: (i) increases in the strengths and intensity of vortices and associated secondary flows ejected from the dimples, as well as (ii) increases in the magnitudes of three-dimensional turbulence production and turbulence transport. The effects of these phenomena are especially apparent in local Nusselt number ratio distributions measured just inside of the dimples, and just downstream of the downstream edges of the dimples.

From the investigations, the results show the superior performance of dimple surface. However, the influence of dimple arrangement on the heat transfer performance has no report on the literature. Therefore, the objective of this study is to observe the thermal characteristic of air flow over flat plate having dimpled surface. In addition, the effect of dimple arrangements, and dimple pitch will be included in this work. The results of this research aim to serve the heat exchanger

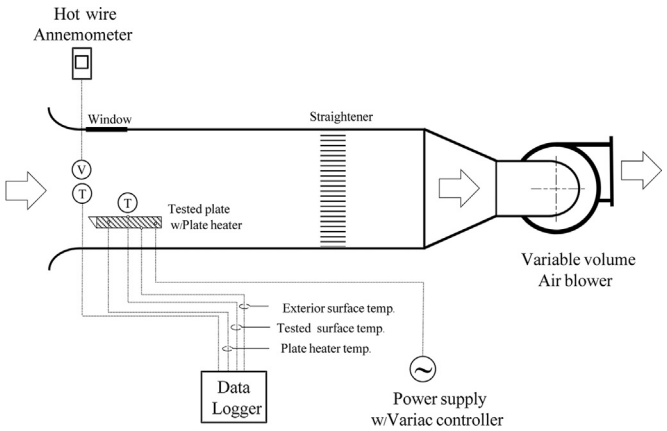

Fig. 1. Schematic diagram of the experimental setup.

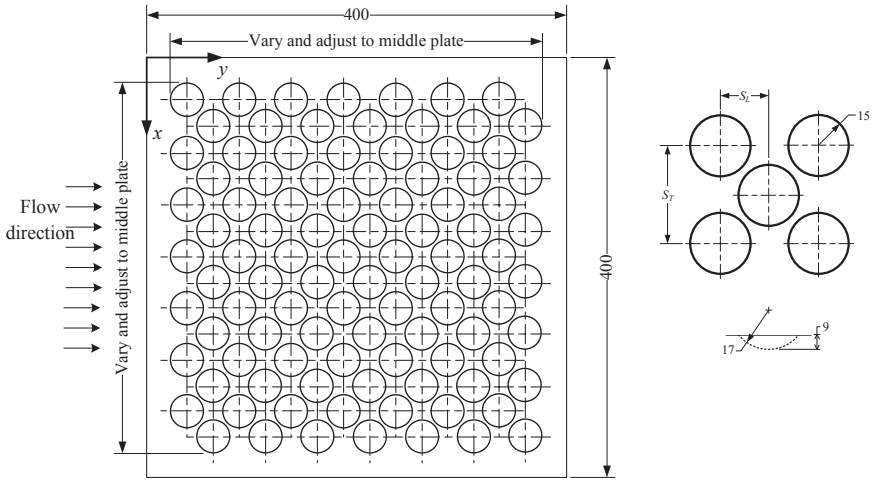

(a) Staggered arrangement

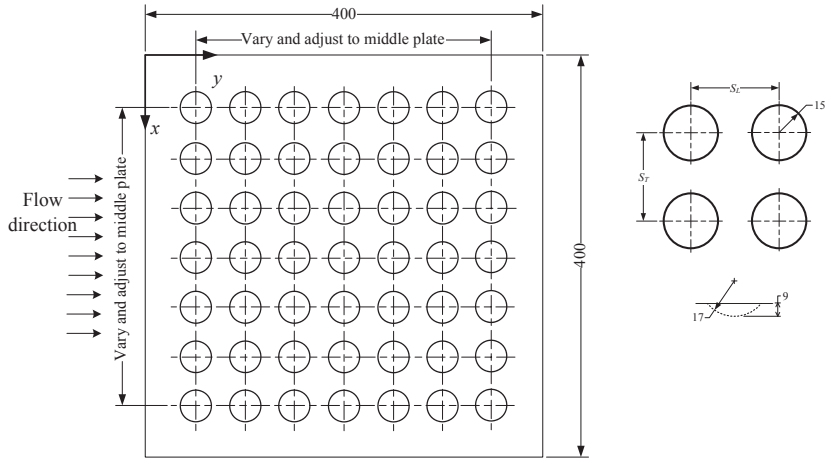

(b) Inline arrangement

Fig. 2. Details of tested surface (all dimensions are in millimeter).

application.

2. Experimental setup and procedure

Fig. 1 presents the schematic sketch of the experimental setup. In this experiment, the laminar and steady-state air flow was obtained. The air stream generated by a centrifugal air blower was flowed over the heated plate with dimples. The temperature of inlet air stream was controlled to about 20 ± 1 °C. The velocity of air stream was controlled by the frequency inverter with the controllable range of 1–5 m/s. The velocity of air stream was measured by a hot wire anemometer with ± 0.2 m/s accuracy. The inlet temperature of air stream was measured by a T-type thermocouple with ± 0.1 °C accuracy. The surface temperature was measured by infrared imaging camera with ± 2 °C accuracy. These temperature was also calibrated surface temperature with T-type thermocouple.

The tested plate was made from 1.5 mm thickness of acrylic. The iron powder was filled beneath the tested plat and the plate electric heater was provided to supply a constant heat flux boundary condition, which the power to the heater was controlled and regulated by a variac power supply to keep the constant average test surface temperature about 50 ± 0.1 °C. All exterior of the test kit were insulated with three layers of 2.5 cm-thickness glass wool insulation to protect the heat loss. It should be noted that the heat flux was calculated from the electrical power supplied to the heater divided by the total surface area (flat portions and dimples surface).

Fig. 2 present the geometric details of the tested surface, including dimpled geometry. The dimple diameter is 30 mm

Table 1
Geometric dimensions of dimpled surface.

No	S_T (mm)	S_L (mm)	Arrangement	S_T/S_L
1	50	25.0	Staggered	2.00
2	50	30.0	Staggered	1.67
3	50	37.5	Staggered	1.33
4	60	25.0	Staggered	2.40
5	60	30.0	Staggered	2.00
6	60	37.5	Staggered	1.60
7	75	25.0	Staggered	3.00
8	75	30.0	Staggered	2.50
9	75	37.5	Staggered	2.00
10	36	36.0	Inline	1.00
11	36	45.0	Inline	0.80
12	36	60.0	Inline	0.60
13	45	45.0	Inline	1.00
14	60	45.0	Inline	1.33

and 9 mm depth. Dimples were employed in an inline and staggered array and Table 1 lists the details of the test samples.

3. Data reduction

The local heat transfer coefficient (h_x) of air flowing over flat plat with dimpled surface can be calculated from

$$h_x = q''_s/(T_s - T_\infty) \tag{1}$$

where q''_s is surface heat flux which is calculated from heat rate level at the tested surface to the total tested surface area (flat portions and dimples surface). T_s is the local surface temperature and T_∞ is the average air stream flowing over the tested plate respectively.

The averaged air side heat transfer coefficient (h) of tested surface is obtained by integrating over the area of tested surface as

$$h = \frac{1}{A_s}\int_{A_s} q''_s/(T_s - T_\infty)dA_s \tag{2}$$

where A_s is tested surface area comprises flat portions and dimples surface.

The averaged Nusselt number (Nu_L) is the ratio of convection to pure conduction heat transfer which is given by

$$Nu_L = \frac{hL}{k_f} \tag{3}$$

where L is maxima stream-wise surface length. For flat plate, L is the length of flat portion. For inline and staggered arrangement, L is the length across the middle of the dimple comprises flat portion and the length along the rim of dimples. k_f is the thermal conductivity of air stream.

It should be noticed that the Reynolds number (Re_L) for this investigation is defined as

$$\mathrm{Re_L} = \frac{\rho_f V_f L}{\mu_f}. \tag{4}$$

where ρ_f, V_f and μ_f are the density of air, the air frontal velocity and the dynamic viscosity of air stream respectively.

All physical properties of air are evaluated at a mean boundary layer temperature (film temperature).

4. Results and discussion

4.1. Validation of the experiment

The validation of the experiment was conducted in this research. The heat transfer from plain flat plate was observed. As the testing condition, the air flow was laminar flow, $\mathrm{Pr} \geq 0.6$ (in general, the Pr of air at 300 K is 0.707) and the test surface was a uniform surface heat flux, it may be show that [8]

$$Nu_\mathrm{L} = 0.68\mathrm{Re}_L^{1/2}Pr^{1/3}. \tag{5}$$

where Pr is the Prandtl number of air stream

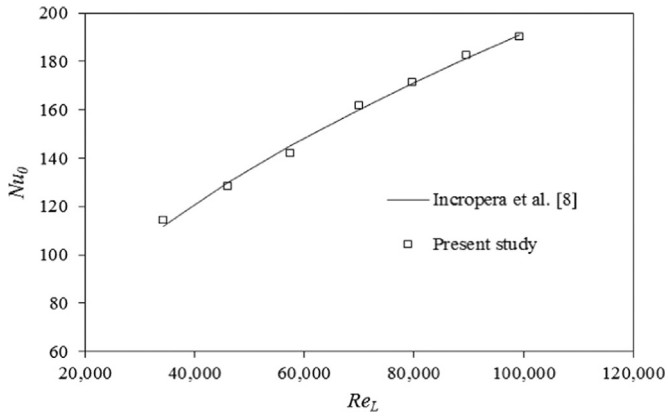

Fig. 3. Comparison of the Nusselt number under the constant heat flux condition from the experimental and the model in case of plain flat plate.

The result of this part was compared with that correlation in finding out the reliability and the accuracy of the experiment. From the experiment, the results show that the surface temperature slightly increases from the entrance about 10 °C along the steam-wise portion. The film temperature are evaluated to obtain the fluid properties, Prandtl number, and Reynolds number. The Nusselt number were calculated by Eqs. (1)–(3). Fig. 3 shows the comparison of Nusselt number from this experiment and that compute by Eq. (5) at various air stream frontal velocity. It should be notice that the data from the experiment agrees very well with the model. Consequently, the experimental setup for this work is reliable and can be applied to the heat transfer experiment in case of the dimpled surface.

4.2. Case of staggered arrangement

In this study, the temperature distribution on the dimpled surface plate was observed by using the infrared imaging camera. The example of result is shown in Fig. 4 which illustrates the temperature distribution along the tested surface of Geometric No. 1. The bulk flow stream direction is from the left hand side. It is found that the dimples surface temperature is higher than that of plain surface. These results come from the recirculation of air stream in the dimpled. It destroys the boundary layer and augment the heat transfer as explain by Mahmood et al. [4]. Moreover, it is found that in each dimpled, the temperature of upstream side is higher than that of the downstream. It means that the heat transfer of upstream halve is lower than the downstream halve. Similar result was also observed by Mahmood et al. [4]. The lowest temperature of dimpled is observed near the diagonal and the downstream edge which the vortex of air stream is generated. Contradict to the results of dimples surface temperature, in case of flat portion, it is found that the surface temperature gradually increases along the downstream. This result may be come from the increasing of air stream temperature along the plate length.

In the case of staggered arrangement, there are nine samples as shown in Table 1. Fig. 5 shows the effect of dimple pitch of the staggered arrangement of the air side heat transfer performance. Results are termed as Nusselt number vs. Reynolds number. As seen in the figure, Nusselt number values are augmented at all Reynolds number and all dimple pitches compared to the flat plate. The Geometric No. 2 yields the highest Nusselt number around 26% better than the flat plate, and Geometric No. 1, No. 7 and No. 9 yield the lowest Nusselt number. It should be noted that higher heat transfer enhancement is observed in case of $S_T/S_L \leq 2.0$. From Geometric No. 1, No. 5 and No. 9, the results show that the Nusselt number increases as S_T increases from 50 to 60 mm and then it decreases as S_T increases from 60 to 75 mm. However, the vortex generation of

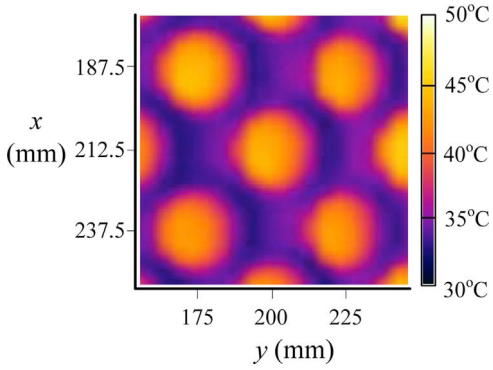

Fig. 4. Temperature distributions of Geometric No. 1 at frontal velocity=4.1 m/s.

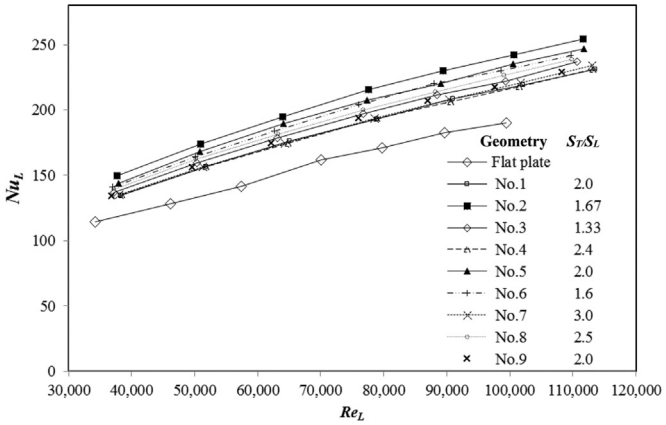

Fig. 5. Effect of dimple arrangement on heat transfer coefficient for staggered arrangement.

downstream dimpled row may be disturbed by that of upstream row. Therefore, the heat transfer augmentation of the shorter S_L may be lower than that of the longer. Consequently, the experimental result shows that higher heat transfer enhancement is observed in case of low S_T/S_L, which, in the literature [4–7], they studied only one dimple arrangement that is $S_T/D=1.62$ and $S_L/D=0.81$ ($S_T/S_L=2.0$).

4.3. Case of Inline arrangement

Fig. 6 presents the temperature distribution on tested surface of Geometric No. 11. The bulk flow direction is from left to right and the dimples are located nearly in each circular temperature distribution. The same temperature distributed trend with the staggered arrangement is found. The temperature values are highest in the upstream halves of the dimples and decrease progressively along the downstream of the dimples, which then become lowest near the diagonal and downstream edges.

In the case of inline arrangement, results are termed as Nusselt number vs. Reynolds number are shown in Fig. 7. As seen in the figure, Nusselt number values are augmented at all frontal velocities and all dimple pitches, which the Geometric No. 14 yield the highest values about 25% better than flat plate, and Geometric No. 12 yields the lowest heat transfer coefficient. From Geometric No. 10 and No. 13, the results show that the Nusselt number increases as S_T increases. It should be noted that the pitch ratio (S_T/S_L) for this case is between 0.6 and 1.33 which lower than that of staggered case. From Fig. 7, it should be noted that the higher S_T/S_L obtains the higher Nusselt number.

4.4. Empirical correlation

From the previous results and discussions, the test data yield the complex behaviors about the heat transfer characteristics that no single curve can be expected to describe in both inline and staggered arrangements. For easier calculations, the multiple linear regression technique is performed to obtain the relevant correlations. The corresponding correlations are given as follows:

Correlation of the Nusselt numbers for the staggered arrangement:

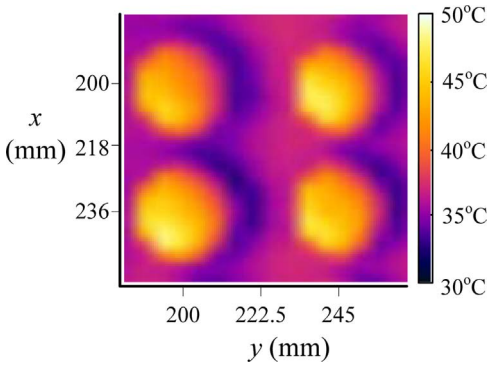

Fig. 6. Temperature distributions of Geometric No. 11 at frontal velocity is 4.1 m/s.

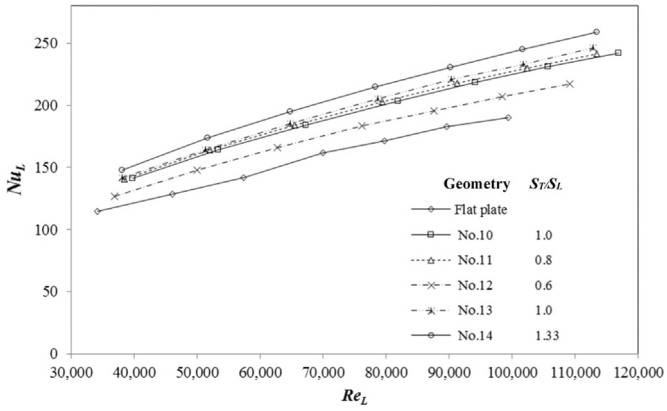

Fig. 7. Effect of dimple arrangement on heat transfer coefficient for inline arrangement.

$$\frac{Nu_L}{Nu_0} = 1.2341\left(\frac{S_L}{S_T}\right)^{0.0827}\left(\frac{S_T}{D}\right)^{0.0206} \tag{6}$$

Correlation of the Nusselt numbers for the inline arrangement:

$$\frac{Nu_L}{Nu_0} = 1.1853\left(\frac{S_T}{S_L}\right)^{0.1483}\left(\frac{S_T}{D}\right)^{0.0328} \tag{7}$$

Fig. 8 shows the comparison of Nu/Nu_0 of the experimental results with the proposed correlations. For the Nusselt number correlations Eqs. (6) and (7) can predict 93.6% and 97% of the experimental data with $\pm 5\%$. The standard deviation of the correlations Eqs. (6) and (7) are 3.36% and 1.69% respectively.

5. Conclusion

The present study reports the heat transfer performance of air flow over the dimples surface. The effects of dimples pitch and dimples arrangement are examined. On the basis of previous discussions, the following conclusions are made:

1. The air side heat transfer performance is augmented at all frontal velocity and all dimples pitch and arrangement. The heat augmentation is approximately 5–26%.
2. For staggered arrangements, the outstanding augmentation is found when the S_T/S_L lower than 2.0. However, in case of inline arrangement, the result shows the highest heat transfer coefficient at $S_T/S_L = 1.33$.

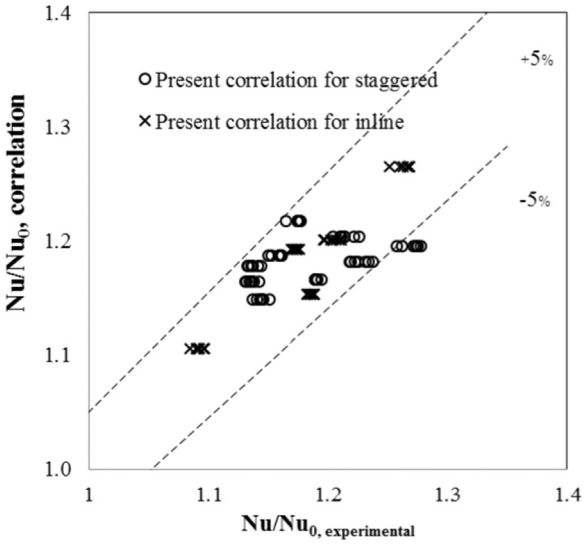

Fig. 8. Comparison of heat transfer correlations with experimental data.

3. Correlations of the present experiment in both staggered and inline arrangement are developed. The proposed correlations yield fairly good predictive ability against the present test data.
4. The vortexes generated by dimple are in three dimensions. The flow structure above the dimple should be further studies.

Acknowledgement

The authors would like to thank the Thermal Technology Research Laboratory at the Mae Moh Training Center Electricity Generating Authority of Thailand for facilitating the testing equipment.

References

[1] Y.P. Chudnovsky, A. Kozlov, Development and Field Trial of Dimpled-Tube Technology for Chemical Industry Process Heaters (Final report), Industrial Technology Program, U.S. Department of Energy, 2006.
[2] V.N. Afanasyev, Y.P. Chudnovsky, A.I. Leontiev, P.S. Roganov, Turbulent flow friction and heat transfer characteristics for spherical cavities on a flat plate, Exp. Therm. Fluid Sci. 7 (1) (1993) 1–8.
[3] M.K. Chyu, Y. Yu, H. Ding, J.P. Downs, F.O. Soechting, Concavity enhanced heat transfer in an internal cooling passage, ASME Paper (1997). (97-GT-437).
[4] G.I. Mahmood, M.L. Hill, D.L. Nelson, P.M. Ligrani, H.K. Moon, B. Glezer, Local heat transfer and flow structure on and above a dimpled surface in a channel, J. Turbomach. 123 (1) (2001) 155.
[5] P.M. Ligrani, J.L. Harrison, G.I. Mahmmod, M.L. Hill, Flow structure due to dimple depressions on a channel surface, Phys. Fluids 13 (11) (2001) 3442–345113.
[6] P.M. Ligrani, N.K. Burgess, S.Y. Won, Nusselt numbers and flow structure on and above a shallow dimpled surface within a channel including effects of inlet turbulence intensity level, ASME Trans. J. Turbomach. 127 (2) (2005) 321–330.
[7] N.K. Burgess, P.M. Ligrani, Effects of dimple depth on channel Nusselt numbers and friction factors, J. Heat. Transf. 127 (1) (2005) 839–847.
[8] F.P. Incropera, D.P. Dewitt, T.L. Bergman, A.L. Lavine, Introduction to Heat Transfer, 5th ed. John Wiley & Sons, 2007.

Nopparat Katkhaw is a Ph.D. student in the Department of Mechanical Engineering, Faculty of Engineering, Chiang Mai University, Thailand. He received M.Eng. in Mechanical Engineering from Chulalongkorn University, Thailand in 2007. His research field covers heat transfer enhancement and eco-energy systems.

Nat Vorayos is an assistant professor in the Department of Mechanical Engineering, Chiang Mai University (CMU), Thailand. He received his Ph.D. (Mechanical Engineering) from Oregon State University, USA. His research activities are thermal system design, heat transfer enhancement and eco-energy systems.

Tanongkiat Kiatsiriroat is a professor in the Department of Mechanical Engineering, Chiang Mai University (CMU), Thailand. He received his D.Eng. in Energy Technology from Asian Institute of Technology in 1987. He worked at King Mongkut's Institute of Technology Thonburi, Bangkok for 16 years before joining CMU in 1995. His research activities are thermal system design, heat transfer enhancement and eco-energy systems.

Atipoang Nuntaphan received B.Eng. and M.Eng. in Mechanical Engineering from Chiang Mai University, Thailand in 1993 and 1997 respectively, and pH.D. in Thermal Technology from School of Energy and Materials, King Mongkut's University of Technology Thonburi, Bangkok, Thailand in 2000. Now he is an engineer of the Electricity Generating Authority of Thailand. His